CAMBRIDGE
UNIVERSITY PRESS

APPLICATION PAPER

Graph characterization of higher-order structure in atmospheric chemical reaction mechanisms

Sam J. Silva[1] and Mahantesh M. Halappanavar[2]

[1]Department of Earth Sciences, The University of Southern California, Los Angeles, CA, USA
[2]Physical and Computational Sciences Directorate, Pacific Northwest National Laboratory, Richland, WA, USA
Corresponding author: Sam J. Silva; Email: samsilva@usc.edu

Abstract

Atmospheric chemical reactions play an important role in air quality and climate change. While the structure and dynamics of individual chemical reactions are fairly well understood, the emergent properties of the entire atmospheric chemical system, which can involve many different species that participate in many different reactions, are not well described. In this work, we leverage graph-theoretic techniques to characterize patterns of interaction ("motifs") in three different representations of gas-phase atmospheric chemistry, termed "chemical mechanisms." These widely used mechanisms, the master chemical mechanism, the GEOS-Chem mechanism, and the Super-Fast mechanism, vary dramatically in scale and application, but they all generally aim to simulate the abundance and variability of chemical species in the atmosphere. This motif analysis quantifies the fundamental patterns of interaction within the mechanisms, which are directly related to their construction. For example, the gas-phase chemistry in the very small Super-Fast mechanism is entirely composed of bimolecular reactions, and its motif distribution matches that of an individual bimolecular reaction well. The larger and more complex mechanisms show emergent motif distributions that differ strongly from any specific reaction type, consistent with their complexity. The proposed motif analysis demonstrates that while these mechanisms all have a similar design goal, their higher-order structure of interactions differs strongly and thus provides a novel set of tools for exploring differences across chemical mechanisms.

Impact Statement

Atmospheric chemistry regulates the abundance and variability of nearly all atmospheric pollutants and many greenhouse gases. These chemical processes are understood to be the result of a highly coupled system of reactions between a large number of chemical species. To model these processes, scientists have developed various "chemical mechanisms," which are mathematical and computational representations of this chemical reaction system. These mechanisms are fundamentally composed of individual chemical reactions that are coupled together in a highly nonlinear manner. This coupling process leads to an emergent structure in the system of chemical interactions. To date, that emergent structure has not been well characterized. This work addresses that research gap through the application of novel graph theoretical analyses. By enumerating mechanism motifs or patterns of interaction in the mechanism, we are able to quantify the higher-order structure present in multiple different atmospheric chemical mechanisms. Our analysis provides a novel quantification of emergent structure in chemical mechanisms and a new set of tools for comparing different atmospheric chemical mechanisms currently in use.

1. Introduction

Chemical reaction-driven variability in the composition of the atmosphere is a fundamental control on the modern environmental challenges of air pollution and climate change. These reactions are the dominant source of most pollution in urban areas and the primary loss process for many important greenhouse gases (Seinfeld and Pandis, 2016). As such, a detailed understanding of atmospheric chemical processes is necessary to understand the driving factors behind these modern environmental crises.

In nature, atmospheric chemistry involves at least tens of thousands of chemical species and hundreds of thousands of reactions. To gain an understanding in light of this complexity, a variety of mathematical methods are used to model the chemical reactions in the atmosphere. These methods most commonly take the form of parameterized systems of coupled differential equations that define the chemical dynamics, which are then studied by solving the system from a given initial condition using various integration methods (e.g., Damian et al., 2002). In conjunction with these approaches, recent work has demonstrated the potential for methods from the graph theory literature to provide valuable complementary information on the structure and dynamics of chemical reactions in the atmosphere (Silva et al., 2021; Wiser et al., 2023).

These graph methods are based on analysis of chemical mechanisms—which are statements of all relevant chemical reactions thought to occur in the atmosphere. These mechanisms are treated as a graph (or a network), where chemical species and reactions can be represented as nodes, and their interactions are represented as edges in a graph. Graph analysis of these mechanisms has led to useful scientific results in the atmospheric chemical sciences. Recent work by Silva et al. (2021) demonstrated that insights gained from graph theoretical analysis of these mechanisms are consistent with those from traditional differential equations-based methods. Dobrijevic et al. (1995) used graph methods to identify important reactions in the chemical mechanisms of planetary atmospheres. Wiser et al. (2023) applied novel graph reduction techniques to develop new atmospheric chemical mechanisms for use in global atmospheric models.

These chemical mechanisms are all broadly designed with similar basic building blocks—a set of reactants reacting to form a set of products. Those products and reactants can then participate in further reactions, ultimately creating the highly coupled system present in most atmospheric chemical mechanisms. The emergent structure and dynamics of this complex and highly coupled chemical system can be difficult to characterize. This challenge arises due to the fact that the behavior of any individual chemical species is not fundamentally representative of the behavior of the overall chemical system. Instead, the emergent properties of the entire mechanism arise due to the coupling of species to each other. These complex couplings of species are represented as connectivity (or network structure) in a graph (Wilson, 2010).

Many methods exist to study the connectivity in graphs (e.g., Estrada, 2016). Here, we focus on so-called "motifs" present in the chemical mechanisms. Motifs are statistically significant repeating patterns of connectivity (also known as graphlets or subgraphs) within the larger graph structure, sometimes termed "fundamental building blocks" of complex systems (e.g., Milo et al., 2002; Masoudi-Nejad et al., 2012). Tracking the relative abundance of a particular motif in a graph can yield insight into larger-scale graph connectivity patterns, and ultimately, the properties of the system being modeled by the graph (Yeger-Lotem et al., 2004; Gonen and Shavitt, 2009; Simmons et al., 2019; Blokhuis et al., 2020). For example, Milo et al. (2002) demonstrated how motifs represent basic processes in graphs of complex systems like food webs, neural circuitry, and gene transcription networks. Alon (2007) reviews the use of these motifs for studying gene and protein transcription networks, demonstrating how a motif-based graph analysis can help characterize the function of processes in these networks. In a chemical context, Tyson and Novák (2010) study motifs in graphs of biochemical reactions, finding that the statistically significant motifs correspond to chemical regulation processes in the system. Blokhuis et al. (2020) derive motifs necessary for catalysis and autocatalysis in chemical reaction mechanisms, underscoring the key role characterizing graph motifs can play in the chemical sciences.

In this work, we explored network motifs across atmospheric chemical mechanisms of varying complexity. For each mechanism, we counted all motifs containing three nodes and compared their

abundance to a structurally similar randomized baseline. Our results illustrate key emergent structural properties of these mechanisms and help explain differences in the dynamical predictions of these three representations of the atmospheric chemical system.

2. Graph representation of atmospheric chemical mechanisms

Chemical reaction mechanisms can be represented as a graph in a variety of ways (Sakamoto et al., 1988; Bajczyk et al., 2018; Wiser et al., 2023). As a brief overview, a graph $G = (V, E)$, is a pair consisting of a set of unique entities represented as nodes or vertices in V, and a set of binary relations on nodes represented as edges in E. A directed graph is a graph where edges are directed or ordered between nodes. A bipartite graph is a graph where the node set can be partitioned into two subsets, such that edges can only exist between nodes in each subset and never within nodes of the same subset. Here, we use the directed bipartite "species-reaction graph" framework (Feinberg, 2019; Silva et al., 2021). In a species reaction graph, there are two classes of nodes: species and reactions. Species nodes are connected to reaction nodes with a directed edge, representing reactions the species participates in as a reactant. Reaction nodes are connected to species that are a product of that reaction by a directed edge. This is summarized in Figure 1 for a hypothetical bimolecular reaction: A + B → C + D.

While the species reaction graph in Figure 1 contains edges with directional arrows pointing only in one direction, these edges can be bidirectional. Bidirectional (or "reciprocal") edges do occur in atmospheric chemical mechanisms, where they are often used to approximate several chemical reactions in one reaction step. An analog to Figure 1 with these bidirectional edges is shown in the Supplementary Material (Figure S1).

We explored three different gas-phase chemical mechanisms in this work: the master chemical mechanism (MCM) v3.3, the GEOS-Chem v12.6 Tropchem chemical mechanism, and the Super-Fast mechanism. Each of these mechanisms aims to reproduce the dynamics of the atmospheric chemical system, though they are designed for very different use cases. The MCM is designed to represent chemical reactions in the atmosphere at a very high level of detail. It has 5833 chemical species and 17,224 reactions (Jenkin et al., 2003; Saunders et al., 2003; Bloss et al., 2005). The MCM is very computationally expensive and is primarily used as a 1-D box model to simulate chemical timescales of hours to days (Jenkin et al., 1997). The GEOS-Chem mechanism represents an intermediate complexity chemical mechanism, with approximately 195 chemical species and 417 reactions (Mao et al., 2013; Sherwen et al., 2016; Travis et al., 2016). GEOS-Chem is typically used to simulate the 3D composition of the atmosphere on regional to global scales, for timescales of up to several years (Bey et al., 2001). The Super-Fast mechanism is a highly parameterized simplified mechanism with 18 chemical species and
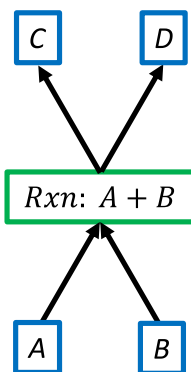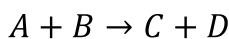
$$A + B \rightarrow C + D$$

Figure 1. *Sample graph of a single bimolecular reaction.*

20 reactions (Cameron-Smith et al., 2006). The orders of magnitude reduction in complexity make Super-Fast the least computationally expensive mechanism studied here, enabling use cases in global 3D climate models with simulation timescales of decades to centuries (Cameron-Smith et al., 2006; Brown-Steiner et al., 2018). In the graph representation of these mechanisms, Super-Fast has 38 nodes and 81 edges, the GEOS-Chem mechanism has 612 nodes and 2444 edges, and the MCM has 23,057 nodes and 57,245 edges. Full visualization and an initial graph theoretical comparison of the bipartite graphs of these three mechanisms can be found in Silva et al. (2021).

3. Motif counting

Motifs are repeating patterns of connectivity (also known as subgraphs or graphlets) within a larger graph. Here, we investigate the smallest possible set of motifs, those containing only three nodes. As in other studies of motifs (Milo et al., 2002; Masoudi-Nejad et al., 2012), we require a motif to have at least two edges (i.e., no isolated nodes). Additionally, since the networks we are studying are all bipartite graphs, there cannot be a 3-node motif with three edges (i.e., a complete triangle), as that would require either species to interconnect or reactions to interconnect. With those qualifications, there are six potential combinations of nodes and edges that form motifs, each distinguished by the directionality of the edges. These six different combinations are often referred to as "isomorphism classes" in the literature (e.g., Milo et al., 2002; Pržulj, 2007), a term that we will use for the remainder of this manuscript. For each isomorphism class, there are two different subgraphs, one where the apex is a species ("species-centered") and one where the apex is a reaction ("reaction-centered"). All possible three-node motifs for directed bipartite graphs, along with what they represent in chemical mechanisms, are shown in Figure 2. Example graphs containing an isomorphism class with bidirectional edges (i.e., those in classes 3, 5, and 6) are shown in the Supplementary Material (Figure S1).

As a baseline example of motif counting, all motifs in the bimolecular reaction in Figure 1 are shown in Figure 3. Isomorphism class 1 appears once in this graph, as the two species react. Isomorphism class 2 appears four times, from reactants reacting to form products. Lastly, isomorphism class 4 appears once as the reaction produces multiple products. In a bipartite reaction with n products, isomorphism class 1 appears once, isomorphism class 2 scales as $2n$, and isomorphism class 4 scales as $n(n-1)/2$. Given that scaling, and so long as there are fewer than five products, a bimolecular reaction graph will have more class 2 motifs than class 4, and only one class 1 motif.

We use the igraph software package (Csardi and Nepusz, 2006) in this work for all graph analysis tasks, including motif counting.

4. Results and discussion

We count and intercompare the motif prevalence in the Super-Fast, GEOS-Chem, and MCM chemical mechanisms. The total motif counts are summarized in the histograms in Figure 4. This motif count scales with the size of the mechanisms, with the large MCM having upwards of 5 orders of magnitude more total motifs than the compact Super-Fast mechanism.

In general, isomorphism classes 1, 2, and 4 are the most common in all three mechanisms. These are the basic building blocks of a bimolecular reaction and are all present in a basic bimolecular reaction with two products, $A + B \rightarrow C + D$, as shown in Figure 3. The other three classes (classes 3, 5, and 6) present in Figure 4 all have bidirectional edges, indicating reciprocal reactions (reactions where some subset of reactants are also products). These are substantially less common because reciprocal reactions are so rare in these reaction mechanisms. Our prior work quantified that only up to 10% of edges are bidirectional (Silva et al., 2021).

A bimolecular reaction generally contributes more motifs in isomorphism class 2 than classes 1 or 4. These mechanisms are dominantly composed of bimolecular reactions, where there are 18 bimolecular reactions (90% of all reactions) in the Super-Fast mechanism, 346 (83%) in the GEOS-Chem mechanism, and 9794 (57%) in the MCM. The Super-Fast motif distribution is consistent with this bimolecular

Isomorphism Class	Reaction-Centered	Species-Centered
1	Two species reacting	Two reactions forming the same species
2	Species reacting to form another species	Species as the product and reactant in separate reactions
3	Reaction with one of the two reactants also a product	Species formed by multiple reactions. In one reaction, the species is both a reactant and a product.
4	A reaction with multiple products.	A species participating in multiple reactions as a reactant.
5	A reaction with multiple products, one of which is also a reactant.	Species reacts to form another species. The species is both a reactant and a product.
6	A reaction with multiple reactants that are also products.	A species formed by multiple reactions where it is both a reactant and a product.

Figure 2. *All possible 3-node motif isomorphism classes are studied in this work, along with species- and reaction-centered chemical explanations.*

reaction motif occurrence pattern. However, the most common isomorphism class in the GEOS-Chem and MCM graphs is isomorphism class 1. Isomorphism class 1 is only present once in any bimolecular reaction and scales with the number of reactants in a reaction as $m(m - 1)/2$, where m is the number of reactants. Since most reactions have a reasonably small number of unique reactants (e.g., ~2), the only way isomorphism class 1 can dominate in the mechanism arises from the connectivity pattern in the graph —namely that many chemical species are reactants and products in more than one reaction.

Certain species in the chemical mechanisms participate in an outsized fraction of all chemical reactions. We investigate what fraction of the motif pattern in Figure 4 is related to the species that participate in the most reactions (i.e., with highest degree), namely the HO_x (OH and HO_2) and NO_x (NO and NO_2) chemical families. These chemical families represent four species that are highly
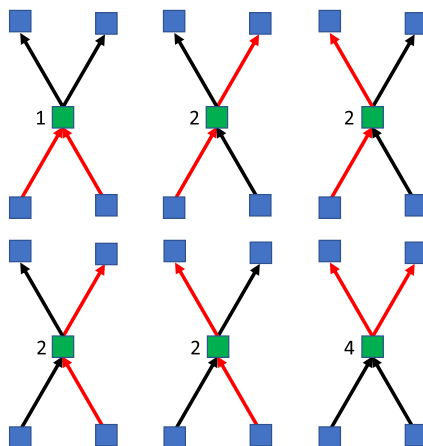
Figure 3. *The three 3-node motifs present in the bimolecular reaction are shown in* Figure 1. *Motifs are shown as red arrows, and their motif isomorphism classes are labeled (see* Figure 2).
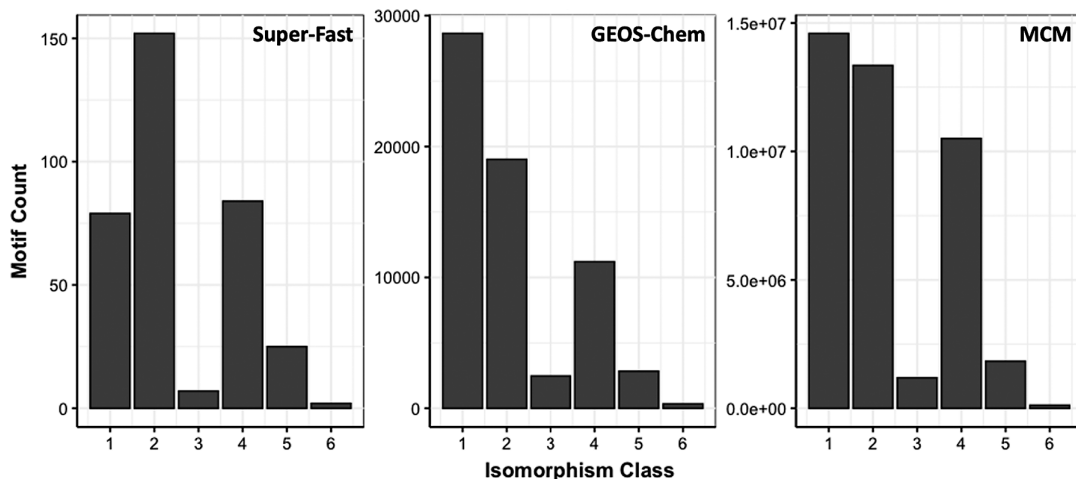

Figure 4. *Distribution of motifs for all six isomorphism classes across all three chemical mechanisms studied in this work.*

connected in these graphs, participating in the bulk of the individual chemical reactions (Silva et al., 2021). The fraction of each isomorphism class attributable to motifs centered on HO_x and NO_x is shown in Figure 5. Motifs centered on the HO_x and NO_x chemical families represent more than 50% of most isomorphism classes. As the mechanism complexity increases, the fraction of motif classes centered on the HO_x and NO_x chemical families increases. The MCM shows nearly 100% of the isomorphism classes containing bidirectional edges (classes 3, 5, and 6) are centered on the HO_x and NO_x chemical families. This indicates that in the MCM, and to a lesser extent GEOS-Chem, nearly all reactions wherein a reactant is also a product are reactions that involve at least one of: OH, HO_2, NO, or NO_2 as that reactant.

We further assess the motif prevalence in the graphs by comparison to the motif prevalence of structurally similar but randomly generated baseline graphs. For a useful 1:1 comparison, these random baselines must retain similar properties as the original graph being studied. To that end, we generated random graphs that were bipartite, had the same number of nodes and edges, and the same degree distribution of chemical species (both in and out degree) as the original chemical mechanism graphs. This
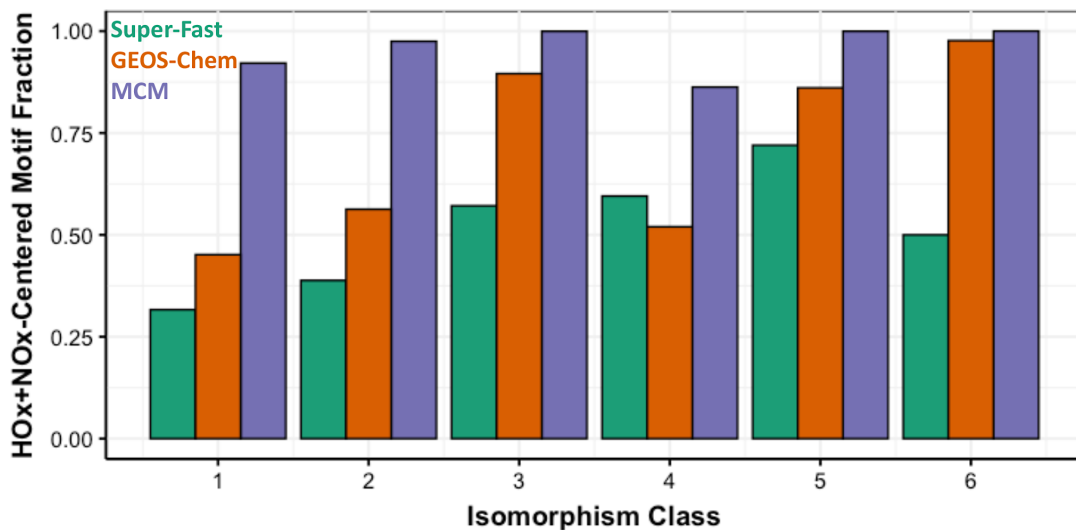
Figure 5. *The fraction of isomorphism classes centered on the HO$_x$ and NO$_x$ chemical families.*

was done by randomly shuffling graph edges such that all species nodes have randomly selected reaction nodes as neighbors. We use this edge-shuffling method in lieu of other random graph generative models (e.g., Watts and Strogatz, 1998; Chung and Lu, 2002) to strictly maintain many of the node level connectivity patterns that are characteristic of atmospheric chemical mechanisms (e.g., highly connected oxidants, Silva et al. 2021). We generated 1000 of these random graphs for each of the three chemical mechanisms studied in this work and counted the motifs in each of these baselines. Once the random baseline graphs were generated and motifs counted, we calculated the statistical significance of the motif prevalence through a standard z-score. We consider any motif isomorphism class with a z-score of greater than or equal to 1.96 ($p \leq 0.05$) to be statistically significant.

The motif prevalence z-scores are summarized in Figure 6. Since the size of the three mechanisms studied here varies across several orders of magnitude, the direct comparison of z-scores across
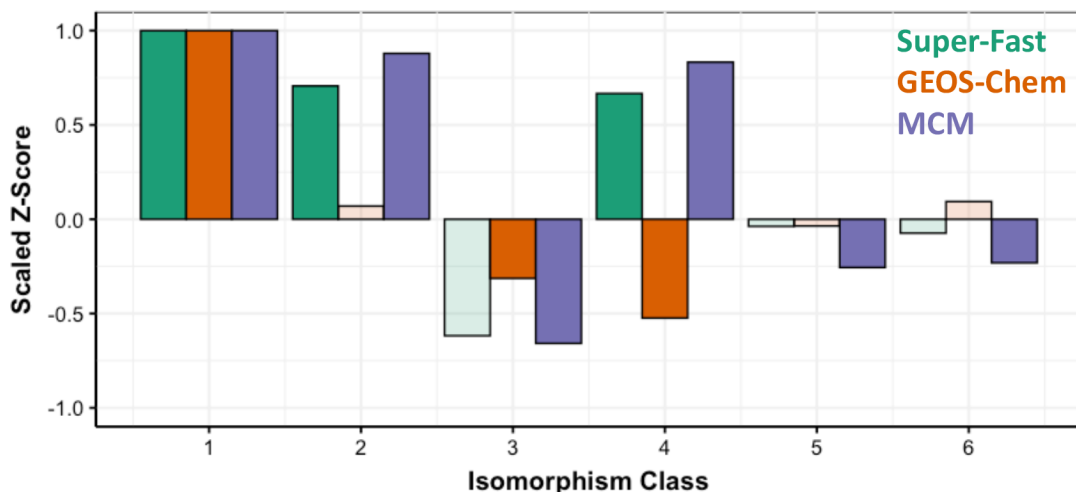

Figure 6. *The scaled z-score of the isomorphism class prevalence in each of the three mechanisms is compared to a random baseline. Transparent bars are not statistically significant.*

mechanisms is not meaningful. As such, we normalize them to the z-score associated with the first isomorphism class. Non-normalized z-scores are shown in the Supplementary Material (Figure S2).

For each of the three mechanisms, the first isomorphism class has the largest associated z-score and is positive (i.e., more likely to occur than in a random baseline graph). This is consistent with the design of these mechanisms wherein multiple chemical compounds react, and multiple reactions form the same compound. Put another way, most chemical species in atmospheric chemical mechanisms participate in multiple chemical reactions. The agreement in prevalence direction and significance across all three chemical mechanisms disappears beyond the first isomorphism class. The MCM and Super-Fast mechanisms all have motif prevalence z-scores that agree directionally, but not all of the Super-Fast z-scores are significant, in contrast to the MCM. Across all three mechanisms, in some cases, the z-score may be in a similar direction (e.g., class 2, 3, and 5), but not all mechanisms have significant class prevalence or wildly different magnitudes. In other cases, the z-score direction may change entirely between chemical mechanisms, as in isomorphism class 4, which is more likely to occur than random in the Super-Fast and MCM mechanisms but less likely in the GEOS-Chem mechanism. The divergent behavior of the GEOS-Chem mechanism with respect to classes 2 and 4 is particularly noteworthy. Along with isomorphism class 1, these are the fundamental three motifs present in a bimolecular reaction and are explicitly added to the mechanisms during construction (see Figure 3). Class 2 is either a species reacting to form another species or species as the product and reactant in separate reactions. In the GEOS-Chem mechanism, isomorphism class 2 is not statistically significantly represented in the connectivity pattern. Isomorphism Class 4, which represents a reaction with multiple products or species participating in multiple reactions as a reactant, is statistically significantly less likely to occur than random in GEOS-Chem, fully opposite from the other two mechanisms. The emergent structure of chemical interactions in these mechanisms differ substantially, despite the fact that all three mechanisms are dominantly composed of biomolecular reactions.

5. A simple model relating motif prevalence to chemical dynamics

Motifs represent fundamental coupling within chemical mechanisms. Since that coupling governs the dynamics of the chemical system, the results in Section 4 raise the question of how differences in motif prevalence impact the dynamics of the three different mechanisms. The three mechanisms investigated here were selected in part because they are so different—they simulate different chemistry, have different species and rate constants, and have very different use cases. As such, attributing any differences in mechanism dynamics to motif prevalence is challenging.

To address this challenge, we use randomly generated graph baselines for the Super-Fast chemical mechanism to illustrate how differences in motif prevalence can lead to differences in dynamical behavior. We convert 1000 random Super-Fast graphs into the system of ODEs they represent and integrate them forward in time. It is important to note that while these random graphs are structurally similar to the true chemical mechanism graph, they do have key differences—principally among them that these graphs are randomly generated, and prior work has shown that chemical mechanisms are decidedly nonrandom (Silva et al., 2021). Further, the randomized reactions are not necessarily chemically plausible—we do not require notions of conservation laws present in the random graphs (e.g., Liu et al., 2024), and we do not limit the number of connected components in the graphs. Given these caveats, we treat these random mechanism baselines only as an interesting simple model for atmospheric chemical dynamics and leave the generation of random mechanism graphs that are structurally distinct but dynamically consistent to future work. We integrate the random ODEs forward in time with all species having initial concentrations of 10 (arbitrary units) and all reaction rates equal to 1 (arbitrary units). Integration is done using a forward Euler integration scheme for 500 timesteps with a stepsize of 0.0001.

The process by which we generate randomized baseline graphs preserves many of the node-level graph properties (e.g., in- and out-degree distribution). This preservation means that each random graph still has compounds that participate in an outsized fraction of reactions as a product or a reactant. We label the compound that is most connected (e.g., has the highest degree) in the random graphs in this way a
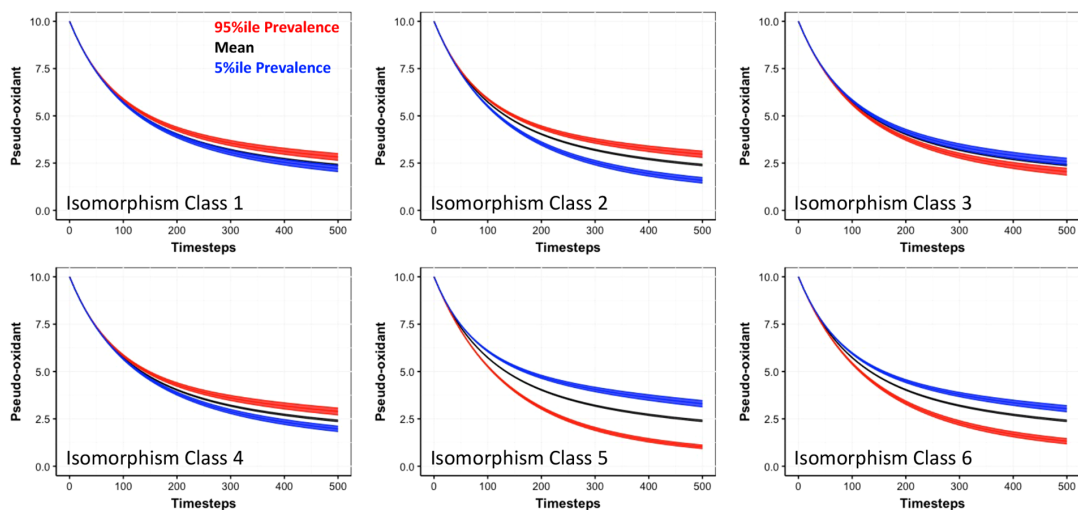
Figure 7. *The mean pseudo-oxidant concentration with time across 1000 random Super-Fast baseline graphs (black line). The mean concentration for the 95%ile and 5%ile for each isomorphism class are shown in red and blue lines, respectively. The standard error of the mean estimate is shown in the shaded areas.*

"pseudo-oxidant." We plot the average concentration of this pseudo-oxidant in the random graphs as a function of time in Figure 7. For each isomorphism class, we additionally plot the average concentration of this pseudo-oxidant for the subset of random graphs with motif prevalence in the top or bottom 5th percentile across random samples. For all three concentration trajectories, we estimate the standard error of the mean as the standard deviation divided by the square root of the number of samples.

Across all of these isomorphism classes, there are two broad categories. The first is those where increased prevalence of the class leads to a slower reduction in pseudo-oxidant concentrations and decreased prevalence of the class leads to a faster concentration reduction. Isomorphism classes 1, 2, and 4 are in this first category. The second is the opposite, where increased prevalence of the class leads to a faster reduction in pseudo-oxidant concentrations, and decreased prevalence of the class leads to a slower concentration reduction. The remaining isomorphism classes 3, 5, and 6 are in this second category. For each isomorphism class after 500 timesteps, the mean pseudo-oxidant concentration is always statistically different from the 95th percentile motif prevalence class and usually different from the 5th percentile class at the 95% confidence interval. The two exceptions are for isomorphism classes 1 and 3, where the pseudo-oxidant concentration for 5th percentile class prevalence is not different than the mean after 500 timesteps.

There are several isomorphism classes that were identified as particularly interesting in the motif prevalence analysis associated with Figure 6, and we highlight the associated pseudo-oxidant behavior in Figure 7 for those classes here. The increased prevalence of isomorphism class 1 is consistent across all three mechanisms, and it arises from two species reacting or two reactions forming the same species in the mechanism. In Figure 7, the increased prevalence of isomorphism class 1 dynamically helps maintain the abundance of this pseudo-oxidant in the atmosphere. The prevalence of isomorphism class 4 is statistically significant for all three mechanisms – underrepresented in GEOS-Chem and overrepresented relative to the baseline in the Super-Fast and MCM graphs. This class comes from reactions with multiple products or species that participate in multiple reactions as a reactant. Dynamically, increased isomorphism class 4 prevalence is associated with a slower pseudo-oxidant loss. In the case of the GEOS-Chem mechanism with reduced prevalence of isomorphism class 4, this simple model indicates that the pseudo-oxidant loss would be modestly faster.

In the three real chemical mechanisms, the pseudo-oxidant analog is OH. Prior work has found different OH concentrations when simulated using these mechanisms (e.g., Brown-Steiner et al., 2018;

Wolfe et al., 2016), though a detailed intercomparison of OH chemical dynamics in these mechanisms has not yet been completed. What is known is that the direction and magnitude of the differences in OH concentrations are strongly dependent on the atmospheric chemical state and cannot be trivially attributed to motif prevalence alone.

6. Summary and broader implications

The higher-order structure in atmospheric chemical mechanisms arises due to the coupling of chemical species through chemical reactions. We quantified this emergent structure by exploring repeating patterns of connectivity known as graph motifs. We counted all 3-node motifs in three mechanisms of varying complexity: the MCM, GEOS-Chem, and the Super-Fast chemical mechanisms. These chemical mechanisms are largely constructed through coupling many individual (largely bimolecular) reactions together. That signature of bimolecular chemistry is present to some degree in the motif counts for each mechanism. However, we find substantial differences in motif class counts across the three mechanisms studie here. The total motif abundance in each mechanism is more complex than simply chaining a series of bimolecular reactions together, consistent with the high degree of chemical coupling and complexity present in atmospheric chemical mechanisms.

Overall, these results point to the fact that while there are some similarities between these chemical mechanisms (they are all simulating the same general system), higher-order structural analysis indicates that they are fundamentally different. This is consistent with the notion that these chemical mechanisms have different patterns of chemical interactions and represent a different set of underlying chemical dynamics (e.g., Brown-Steiner et al., 2018).

Graph structural analysis can provide key insight to enable detailed comparison and diagnosis of system behavior across the atmospheric and environmental sciences. Future work integrating additional processes into these graph mechanism representations (e.g., photolysis, heterogeneous chemistry, etc.) and work further exploring the direct connection between graph structural properties and dynamical system behavior would be valuable. This would provide additional context for interpreting the implications of the differences shown in this comparative analysis.

References

Alon U (2007) Network motifs: theory and experimental approaches. *Nature Reviews Genetics* **8**(6), 450–461. https://doi.org/10.1038/nrg2102.

Bajczyk MD, Dittwald P, Wołos A, Szymkuć S, Grzybowski BA (2018) Discovery and enumeration of organic-chemical and biomimetic reaction cycles within the network of chemistry. *Angewandte Chemie International Edition* **57**(9), 2367–2371. https://doi.org/10.1002/anie.201712052.

Bey I, **Jacob DJ**, **Yantosca RM**, **Logan JA**, **Field BD**, **Fiore AM**, et al. (2001) Global modeling of tropospheric chemistry with assimilated meteorology: model description and evaluation. *Journal of Geophysical Research: Atmospheres 106*(D19), 23073–23095. https://doi.org/10.1029/2001JD000807.

Blokhuis A, **Lacoste D**, **Nghe P** (2020) Universal motifs and the diversity of autocatalytic systems. *Proceedings of the National Academy of Sciences 117*(41), 25230–25236. https://doi.org/10.1073/pnas.2013527117.

Bloss C, **Wagner V**, **Jenkin ME**, **Volkamer R**, **Bloss WJ**, **Lee JD**, et al. (2005) Development of a detailed chemical mechanism (MCMv3.1) for the atmospheric oxidation of aromatic hydrocarbons. *Atmospheric Chemistry and Physics 5*(3), 641–664. https://doi.org/10.5194/acp-5-641-2005.

Brown-Steiner B, **Selin NE**, **Prinn R**, **Tilmes S**, **Emmons L**, **Lamarque J-F**, **Cameron-Smith P** (2018) Evaluating simplified chemical mechanisms within present-day simulations of the community earth system model version 1.2 with CAM4 (CESM1.2 CAM-chem): MOZART-4 vs. Reduced hydrocarbon vs. super-fast chemistry. *Geoscientific Model Development 11*(10), 4155–4174. https://doi.org/10.5194/gmd-11-4155-2018.

Cameron-Smith P, **Lamarque J-F**, **Connell P**, **Chuang C**, **Vitt F** (2006) Toward an Earth system model: atmospheric chemistry, coupling, and petascale computing. *Journal of Physics: Conference Series 46*, 343–350. https://doi.org/10.1088/1742-6596/46/1/048.

Chung F., **Lu L** (2002) Connected components in random graphs with given expected degree sequences. *Annals of Combinatorics 6*(2), 125–145. https://doi.org/10.1007/PL00012580.

Csardi G, **Nepusz T** (2006) The igraph software package for complex network research. *InterJournal Complex Systems 1695*. https://cran.rproject.org/web/packages/igraph/citation.html.

Damian V, **Sandu A**, **Damian M**, **Potra F**, **Carmichael GR** (2002) The kinetic preprocessor KPP—a software environment for solving chemical kinetics. *Computers & Chemical Engineering 26*(11), 1567–1579. https://doi.org/10.1016/S0098-1354(02)00128-X.

Dobrijevic M, **Parisot JP**, **Dutour I.** (1995) A study of chemical systems using signal flow graph theory: application to Neptune. *Planetary and Space Science 43*(1), 15–24. https://doi.org/10.1016/0032-0633(94)00147-J.

Estrada E. (2016) *The Structure of Complex Networks: Theory and Applications*. Oxford: Oxford University Press.

Feinberg M. (2019) The species-reaction graph. In Feinberg M (ed.), *Foundations of Chemical Reaction Network Theory*, Vol. *202*. Cham: Springer International Publishing, pp. 205–240. https://doi.org/10.1007/978-3-030-03858-8_11.

Gonen M., **Shavitt Y.** (2009) Approximating the number of network motifs. In: Avrachenkov K., Donato D., Litvak N., (eds) *Algorithms and Models for the Web-Graph. WAW 2009. Lecture Notes in Computer Science*, vol *5427*. Springer, Berlin, Heidelberg. https://doi.org/10.1007/978-3-540-95995-3_2

Jenkin ME, **Saunders SM**, **Pilling MJ** (1997) The tropospheric degradation of volatile organic compounds: a protocol for mechanism development. *Atmospheric Environment 31*(1), 81–104. https://doi.org/10.1016/S1352-2310(96)00105-7

Jenkin ME, **Saunders SM**, **Wagner V**, **Pilling MJ** (2003) Protocol for the development of the master chemical mechanism, MCM v3 (Part B): tropospheric degradation of aromatic volatile organic compounds. *Atmospheric Chemistry and Physics 3*(1), 181–193. https://doi.org/10.5194/acp-3-181-2003.

Liu Z, **Sturm PO**, **Bharadwaj S**, **Silva SJ**, **Tegmark M** (2024) Interpretable conservation laws as sparse invariants. *Physical Review E 109*(2), L023301. https://doi.org/10.1103/PhysRevE.109.L023301.

Mao J, **Paulot F**, **Jacob DJ**, **Cohen RC**, **Crounse JD**, **Wennberg PO** et al. (2013) Ozone and organic nitrates over the eastern United States: sensitivity to isoprene chemistry. *Journal of Geophysical Research: Atmospheres 118*(19), 2013JD020231. https://doi.org/10.1002/jgrd.50817.

Masoudi-Nejad A, **Schreiber F**, **Kashani ZRM** (2012) Building blocks of biological networks: a review on major network motif discovery algorithms. *IET Systems Biology 6*(5), 164–174. https://doi.org/10.1049/iet-syb.2011.0011.

Milo R, **Shen-Orr S**, **Itzkovitz S**, **Kashtan N**, **Chklovskii D**, **Alon U** (2002) Network motifs: simple building blocks of complex networks. *Science 298*(5594), 824–827. https://doi.org/10.1126/science.298.5594.824.

Pržulj N (2007) Biological network comparison using graphlet degree distribution. *Bioinformatics 23*(2), e177–e183. https://doi.org/10.1093/bioinformatics/btl301.

Sakamoto A, **Kawakami H**, **Yoshikawa K** (1988) A graph theoretical approach to complex reaction networks. *Chemical Physics Letters 146*(5), 444–448. https://doi.org/10.1016/0009-2614(88)87475-X.

Saunders SM, **Jenkin ME**, **Derwent RG**, **Pilling MJ** (2003) Protocol for the development of the master chemical mechanism, MCM v3 (Part A): tropospheric degradation of non-aromatic volatile organic compounds. *Atmospheric Chemistry and. Physics 3* (1), 161–180. https://doi.org/10.5194/acp-3-161-2003.

Seinfeld J.H., **Pandis S.N.** (2016) *Atmospheric Chemistry and Physics: From Air Pollution to Climate Change*, 3rd Edn. Hoboken, NJ: Wiley.

Sherwen T, **Schmidt JA**, **Evans MJ**, **Carpenter LJ**, **Großmann K**, **Eastham SD**, et al. (2016) Global impacts of tropospheric halogens (Cl, Br, I) on oxidants and composition in GEOS-Chem. *Atmospheric Chemistry and Physics 16*(18), 12239–12271. https://doi.org/10.5194/acp-16-12239-2016.

Silva SJ, **Burrows SM**, **Evans MJ**, **Halappanavar M** (2021) A graph theoretical intercomparison of atmospheric chemical mechanisms. *Geophysical Research Letters 48*(1), e2020GL090481. https://doi.org/10.1029/2020GL090481.

Simmons BI, **Cirtwill AR**, **Baker NJ**, **Wauchope HS**, **Dicks LV**, **Stouffer DB**, **Sutherland WJ** (2019) Motifs in bipartite ecological networks: uncovering indirect interactions. *Oikos 128*(2), 154–170. https://doi.org/10.1111/oik.05670.

Travis KR, **Jacob DJ**, **Fisher JA**, **Kim PS**, **Marais EA**, **Zhu L**, et al. (2016) Why do models overestimate surface ozone in the Southeast United States? *Atmospheric Chemistry and Physics 16*(21), 13561–13577. https://doi.org/10.5194/acp-16-13561-2016.

Tyson JJ, **Novák B** (2010) Functional motifs in biochemical reaction networks. *Annual Review of Physical Chemistry 61*(1) 219–240. https://doi.org/10.1146/annurev.physchem.012809.103457.

Watts DJ, **Strogatz SH** (1998) Collective dynamics of 'small-world' networks. *Nature 393*(6684), 440–442. https://doi.org/10.1038/30918.

Wilson R.J. (2010) *Introduction to Graph Theory*, 5th Edn. Harlow: Pearson/Prentice Hall.

Wiser F, **Place B**, **Sen S**, **Pye HOT**, **Yang B**, **Westervelt DM** et al. (2023) AMORE-Isoprene v1.0: a new reduced mechanism for gas-phase isoprene oxidation. *Geoscientific Model Development*, *16*, 1801–1821. https://doi.org/10.5194/gmd-16-1801-2023.

Wolfe GM, **Marvin MR**, **Roberts SJ**, **Travis KR**, **Liao J** (2016) The framework for 0-D atmospheric modeling (F0AM) v3.1. *Geoscientific Model Development 9*(9), 3309–3319. https://doi.org/10.5194/gmd-9-3309-2016.

Yeger-Lotem E, **Sattath S**, **Kashtan N**, **Itzkovitz S**, **Milo R**, **Pinter RY**, et al. (2004) Network motifs in integrated cellular networks of transcription-regulation and protein–protein interaction. *Proceedings of the National Academy of Sciences 101*(16), 5934–5939. https://doi.org/10.1073/pnas.0306752101.